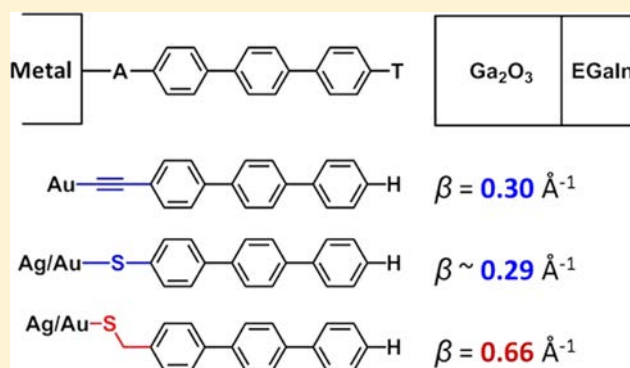


## Tunneling across SAMs Containing Oligophenyl Groups

Carleen M. Bowers,<sup>†</sup> Dmitriy Rappoport,<sup>†</sup> Mostafa Baghbanzadeh,<sup>†</sup> Felice C. Simeone,<sup>†</sup>  
Kung-Ching Liao,<sup>†</sup> Sergey N. Semenov,<sup>†</sup> Tomasz Żaba,<sup>‡</sup> Piotr Cyganik,<sup>‡</sup> Alan Aspuru-Guzik,<sup>†</sup>  
and George M. Whitesides<sup>\*,†,§</sup><sup>†</sup>Department of Chemistry and Chemical Biology, Harvard University, 12 Oxford Street, Cambridge, Massachusetts 02138, United States<sup>‡</sup>Smoluchowski Institute of Physics, Jagiellonian University, ul. Lojasiewicza 11, 30-348 Krakow, Poland<sup>§</sup>Kavli Institute for Bionano Science & Technology, School of Engineering and Applied Sciences, Harvard University, 29 Oxford Street, Cambridge, Massachusetts 02138, United States

## Supporting Information

**ABSTRACT:** This paper reports rates of charge tunneling across self-assembled monolayers (SAMs) of compounds containing oligophenyl groups, supported on gold and silver, using Ga<sub>2</sub>O<sub>3</sub>/EGaIn as the top electrode. It compares the attenuation constant,  $\beta$ , and the pre-exponential parameter,  $J_0$ , of the simplified Simmons equation across oligophenyl groups (R = Ph<sub>*n*</sub>; *n* = 1, 2, 3) with three different anchoring groups (thiol, HSR; methanethiol, HSCH<sub>2</sub>R; and acetylene, HC≡CR) that attach R to the template-stripped gold or silver substrate. The results demonstrate that the structure of the molecular linker between the anchoring group (–S– or –C≡C–) and the oligophenyl moiety significantly influences the rate of charge transport. SAMs of SPh<sub>*n*</sub> and C≡CPh<sub>*n*</sub> on gold show similar values of  $\beta$  and  $\log |J_0|$  ( $\beta = 0.28 \pm 0.03 \text{ \AA}^{-1}$  and  $\log |J_0| = 2.7 \pm 0.1$  for Au/SPh<sub>*n*</sub>;  $\beta = 0.30 \pm 0.02 \text{ \AA}^{-1}$  and  $\log |J_0| = 3.0 \pm 0.1$  for Au/C≡CPh<sub>*n*</sub>). The introduction of a single intervening methylene (CH<sub>2</sub>) group between the anchoring sulfur atom and the aromatic units generates SAMs of SCH<sub>2</sub>Ph<sub>*n*</sub> and increases  $\beta$  to ca.  $0.66 \pm 0.06 \text{ \AA}^{-1}$  on both gold and silver substrates. (For *n*-alkanethiolates on gold, the corresponding values are  $\beta = 0.76 \pm 0.03 \text{ \AA}^{-1}$  and  $\log |J_0| = 4.2 \pm 0.2$ ). Density functional theory calculations indicate that the highest occupied molecular orbitals (HOMOs) of both SPh<sub>*n*</sub> and C≡CPh<sub>*n*</sub> extend beyond the anchoring group and onto the phenyl rings; SAMs composed of these two groups of molecules result in indistinguishable rates of charge transport. The introduction of the CH<sub>2</sub> group, to generate SCH<sub>2</sub>Ph<sub>*n*</sub>, disrupts the delocalization of the orbitals, localizes the HOMO on the anchoring sulfur atom, and results in the experimentally observed increase in  $\beta$  to a value closer to that of a SAM of *n*-alkylthiolate molecules.



## INTRODUCTION

The correlation between the structure of self-assembled monolayers (SAMs) containing *n*-alkyl groups and the rate of charge tunneling in junctions of the form M/A(CH<sub>2</sub>)<sub>*n*</sub>T//Ga<sub>2</sub>O<sub>3</sub>/EGaIn (where M is the metal substrate, A is the anchoring group, and T is the terminal group), is surprisingly straightforward: the length of the insulating –(CH<sub>2</sub>)<sub>*n*</sub>– group, which presents a high tunneling barrier, largely controls the rate of charge transport. The height and shape of this tunneling barrier make the influence of many structural changes at the interfaces (i.e., changes to the anchoring group, A, and the terminal group, T, and their contacts with the top and bottom electrodes) difficult to detect.<sup>1</sup> Among the exceptions are the observation of a small (and still imperfectly understood) “odd–even effect” in charge transport across *n*-alkanethiolates on gold,<sup>2–6</sup> the observation of a reduction in current density (by factors of 20–30) when fluorine is present at the SAM//Ga<sub>2</sub>O<sub>3</sub>

interface,<sup>7</sup> and the observation of rectification of current when T is a redox-active group such as ferrocenyl<sup>6,8,9</sup> or bipyridyl.<sup>10</sup>

As a part of our study of the relation between the structure of the organic groups of SAMs and the rate of charge transfer by tunneling across them, we have examined the relationship between the structure of polyaromatics (molecules that result in a reduction in the height of the tunneling barrier relative to that characterizing aliphatics<sup>11–25</sup>) and the rate of charge transport. We have examined the influence of the chemical structure of the anchoring group and also that of the linker between the anchoring group and the phenyl rings by measuring rates of charge transport across SAMs of oligo(phenyl)thiols (M/SPh<sub>*n*</sub>), oligo(phenyl)methanethiols (M/SCH<sub>2</sub>Ph<sub>*n*</sub>), and oligo(phenyl)acetylenes (M/C≡CPh<sub>*n*</sub>), where *n* = 1–3 and

Received: February 4, 2016

Revised: April 10, 2016

Published: April 11, 2016

M = gold or silver as the metal electrode (Figure 1). Using junctions of the form M/A(Ph)<sub>n</sub>H//Ga<sub>2</sub>O<sub>3</sub>/EGaIn, we

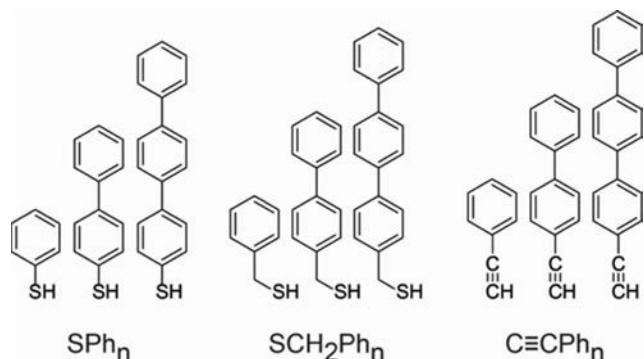


**Figure 1.** Structures of oligo(phenyl)thiols (SPh<sub>n</sub>), oligo(phenyl)methanethiols (SCH<sub>2</sub>Ph<sub>n</sub>), and oligo(phenyl)acetylenes (C≡CPh<sub>n</sub>) used to form SAMs on template-stripped silver and gold substrates (Ag<sup>TS</sup> and Au<sup>TS</sup>, respectively). “Ph” indicates a phenylene ring, and *n* is the number of such rings. For each molecule, we measured the length of the tunneling barrier, *d*, as the distance from the anchoring atom (sulfur or carbon directly coordinated to the metal substrate) to the distal H atom.

compared these rates with rates for length-matched *n*-alkanethiols. Although these SAMs are based on simple oligophenyls and share (we assume) a similar Ph–H//Ga<sub>2</sub>O<sub>3</sub> interface, they differ substantially in their physical and electronic interactions with the metal substrates that form the “bottom” interface (M/A). Our results indicate that SAMs of SPh<sub>n</sub> and C≡CPh<sub>n</sub> on gold (both of which are characterized by the delocalization of high-energy orbitals across the molecule and between the molecule and the electrode<sup>11</sup>) have similar low values of the attenuation factor  $\beta$  and the pre-exponential constant  $J_0$  in the simplified Simmons equation<sup>26</sup> (eq 1),

$$J(V) = J_0(V)e^{-\beta d} = J_0(V)10^{-\beta d/2.303} \quad (1)$$

i.e.,  $\beta = 0.28 \pm 0.03 \text{ \AA}^{-1}$  and  $\log |J_0| = 2.7 \pm 0.1$  for Au/SPh<sub>n</sub> and  $\beta = 0.30 \pm 0.02 \text{ \AA}^{-1}$  and  $\log |J_0| = 3.0 \pm 0.1$  for Au/C≡CPh<sub>n</sub>. The introduction of a single intervening CH<sub>2</sub> group into the S–C bond, which converts SPh<sub>n</sub> to SCH<sub>2</sub>Ph<sub>n</sub>, disrupts the delocalization of the orbitals between the aromatic moiety and the metal electrode<sup>27–29</sup> and increases  $\beta$  to  $0.66 \pm 0.06 \text{ \AA}^{-1}$  and  $\log |J_0|$  to  $4.0 \pm 0.3$ ; these values are surprisingly close to those derived from SAMs of *n*-alkanethiols ( $\beta_{\text{Au}} = 0.76 \pm 0.03 \text{ \AA}^{-1}$  and  $\log |J_0| = 4.2 \pm 0.2$ ).<sup>2</sup>

SAMs of SPh<sub>n</sub> and SCH<sub>2</sub>Ph<sub>n</sub> have been characterized extensively. They form structures that are highly ordered and densely packed on both silver and gold substrates.<sup>30–35</sup> The exception is thiophenol (HSPH), which has been reported to form poorly defined SAMs, possibly because of the weak intermolecular forces between the aromatic rings.<sup>30,31,35</sup> The surface structure of thiolates on metal is the same for SAMs of *n*-alkanethiolates and SAMs of aromatics ( $(\sqrt{3} \times \sqrt{3})R30^\circ$  on gold and  $(\sqrt{7} \times \sqrt{7})R10.9^\circ$  on silver), but the cant angle ( $\alpha$ ) for the aromatics is slightly less than that for the alkanethiolates ( $\alpha \approx 20^\circ$  for SAMs of terphenylthiol on Au and  $\alpha \approx 30^\circ$  for SAMs of *n*-alkanethiols on Au).<sup>30,36</sup> Oligophenyl groups present in a SAM adopt a near-planar conformation and pack in a herringbone structure.<sup>30,37,38</sup>

Characterization of SAMs of C≡CPh<sub>n</sub> on gold indicates that the acetylene group binds in an upright configuration on

gold.<sup>39–42</sup> Cyganik and co-workers demonstrated that it is possible to form highly ordered SAMs of *n*-alkylacetylenes on gold in nonoxidizing environments;<sup>43</sup> the presence of O<sub>2</sub> (before or during SAM formation) leads to poorly organized films and to oxidation of the acetylene group. (See the Supporting Information for experimental details on the formation of the SAMs.)

In measurements of charge transport across a metal–SAM–metal junction, charges encounter a tunneling barrier whose shape is determined by the electrical characteristics of at least five components: the SAM, the two electrodes, and the two interfaces between the SAM and the electrodes. The simplified Simmons equation<sup>26,44,45</sup> (eq 1) parametrizes the rate of charge transport assuming a simple rectangular shape for the tunneling barrier. In this approximation,  $J(V)$  decays exponentially with increasing width of the tunneling barrier, *d*, which is often taken to be the distance between the two electrodes. Here we estimated *d* as the calculated length of the molecule making up the SAM (in Å, from the anchoring atom to the distal hydrogen atom). The Supporting Information summarizes some of the theoretical limitations of this approach.

## RESULTS AND DISCUSSION

Figure 2 summarizes the rates of charge transport, using a conical Ga<sub>2</sub>O<sub>3</sub>/EGaIn tip as the top electrode, across SAMs of oligophenyls having thiol (HS–) and methanethiol (HSCH<sub>2</sub>–) anchoring groups on gold and silver substrates and an acetylene (HC≡C–) anchoring group on gold substrates. (Figures S1 and S2 and Table S2 provide additional details on the measurements). We provide a comparison of  $\beta$  and  $J_0$  for standard *n*-alkanethiolates on gold and silver substrates. For all of the systems, values of  $\log |J|$  (the log-Gaussian mean value of the current density) varied linearly with *d*. Assuming a through-molecule transport mechanism, we approximated *d* as the length of the molecule from the anchoring atom to the distal hydrogen atom (the diagram in Figure 2 shows this approximation of *d*.) Linear regression analyses of the values of  $\log |J|$  versus *d* yielded the values of the log-injection current ( $\log |J_0|$ , from the intercept at the *y* axis) and the tunneling parameter ( $\beta$ , from the slope) for each system (Figure 2).

The rates of charge transport across SAMs of *n*-alkanethiols on gold and silver ( $\beta_{\text{Au}} = 0.76 \pm 0.03 \text{ \AA}^{-1}$  and  $\log |J_{0,\text{Au}}| = 4.2 \pm 0.2$ ;  $\beta_{\text{Ag}} = 0.72 \pm 0.05 \text{ \AA}^{-1}$  and  $\log |J_{0,\text{Ag}}| = 3.6 \pm 0.3$ )<sup>2,46</sup> serve as a reference range against which we correlate the trends in electrical behavior with the changes in molecular and electronic structure. The value of  $J_0$  is indistinguishable for SAMs of SCH<sub>2</sub>Ph<sub>n</sub> and S(CH<sub>2</sub>)<sub>n</sub>CH<sub>3</sub> on both silver ( $\log |J_0| = 3.7 \pm 0.3$  for SCH<sub>2</sub>Ph<sub>n</sub> and  $3.6 \pm 0.3$  for S(CH<sub>2</sub>)<sub>n</sub>CH<sub>3</sub>) and gold ( $\log |J_0| = 4.0 \pm 0.2$  for SCH<sub>2</sub>Ph<sub>n</sub> and  $4.2 \pm 0.2$  for S(CH<sub>2</sub>)<sub>n</sub>CH<sub>3</sub>). Frisbie and co-workers made a similar observation using conducting-probe atomic force microscopy.<sup>47</sup> They reported the same contact resistance ( $R_0$ ) for SAMs of oligo(phenyl)methanethiols and SAMs of *n*-alkanethiols on gold. One possible explanation for the similar values of  $J_0$  is the similarity in the electronic structures of the interfaces between the SAMs and the bottom electrode: both SAMs have a metal/SCH<sub>2</sub>–interface. SAMs of oligophenyls that lack a methylene spacer, here SPh<sub>n</sub> (on gold and silver) and C≡CPh<sub>n</sub> (on gold), give values of  $J_0$  (estimated by extrapolation) that are lower by about a factor of 10 than  $J_0$  observed for *n*-alkanethiolates ( $\log |J_0| = 4.2 \pm 0.2$ ; Figure 2).

The measurement and interpretation of the parameter  $J_0$  in the simplified Simmons equation<sup>26,44,45</sup> (eq 1) are both

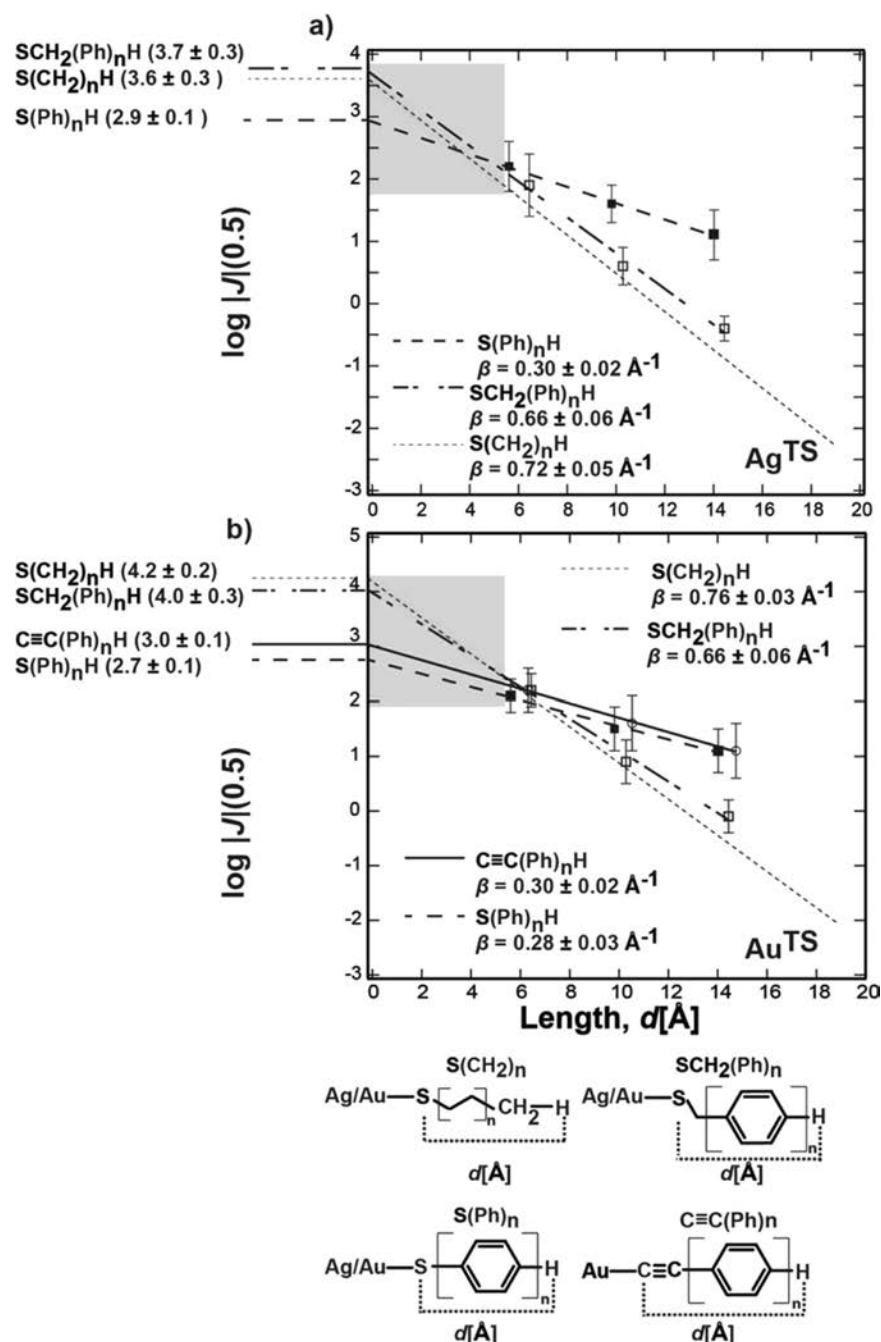


**Figure 2.** Plots of the Gaussian mean values of  $\log |J|$  at +0.5 V vs molecular length  $d$  (in Å) for SAMs on (a) Ag<sup>TS</sup> and (b) Au<sup>TS</sup>. The value of  $d$  (shown by the dotted lines at the bottom) was calculated as the distance from the anchoring atom, which is bound covalently to the bottom electrode, to the distal hydrogen atom, which is in van der Waals contact with the Ga<sub>2</sub>O<sub>3</sub>/EGaIn electrode, under the assumption of an all-trans extended conformation. The gray box in each panel indicates the region over which the data must be extrapolated to estimate  $J_0(V)$  at  $d = 0$ . Since the structural elements in this region differ from those in the region where there are data (the region of Ph<sub>n</sub>), extrapolation may be inappropriate for S(Ph)<sub>n</sub> and C≡C(Ph)<sub>n</sub>, although the correctness of this extrapolation is well-validated for  $n$ -alkanethiolates on gold and silver.<sup>2,49</sup>

complicated. The value of  $J_0$  (determined by extrapolation of the best-fit line to  $d = 0$ ) across aromatics has been less discussed than that for  $\beta$ , in substantial part because of differences in the reported values of  $J_0$  across techniques. The Supporting Information lists some of the issues that make this empirical parameter difficult to interpret. Given the difficulties in interpreting  $J_0$ , we focus our analysis on  $\beta$ .

Measurements of charge tunneling across SAMs of SPh<sub>n</sub> with  $n$  increasing from 1 to 3 yielded  $\beta_{\text{Ag}} = 0.30 \pm 0.02 \text{ \AA}^{-1}$  and  $\beta_{\text{Au}} = 0.28 \pm 0.03 \text{ \AA}^{-1}$  (Figure 2); these values agree with previous

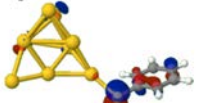
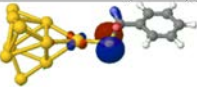
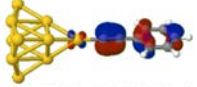
experimental reports using single-molecule and large-area junctions.<sup>15,16,34,48–53</sup> The results presented here also agree with theoretical calculations by Ratner and co-workers;<sup>11</sup> using density functional theory (DFT), those authors predicted a  $\beta$  value of ca.  $0.3 \text{ \AA}^{-1}$  for SAMs of poly(phenyl)dithiolates by assuming continuous conjugation of the molecules with the metal electrodes.

We compared the electrical properties of SAMs of SPh<sub>n</sub> to SAMs of C≡CPh<sub>n</sub> on Au<sup>TS</sup> (Figure 2b). Both molecular systems are conjugated (i.e., the  $\pi$  electrons are delocalized

across the molecular backbone), but they differ by the chemical structure of the anchoring group ( $-S-$  vs  $-C\equiv C-$ ). The values of  $\beta$  for these two series of SAMs are indistinguishable ( $\beta = 0.28 \pm 0.03 \text{ \AA}^{-1}$  for  $\text{Au}/\text{SPh}_n$  and  $\beta = 0.30 \pm 0.02 \text{ \AA}^{-1}$  for  $\text{Au}/\text{C}\equiv\text{CPh}_n$ ).

To help correlate the experimental measurements of the rate of charge transport with changes in the molecular structure of the SAM at the interface, we performed DFT calculations of the electronic structures of the series of molecules studied here (Tables 1 and S3–S5). The computational details are given in

**Table 1.  $\alpha$  (Spin-Up) Orbital Energies (in eV) and Shapes of the High-Lying Occupied Molecular Orbitals of the Anchoring Groups Oriented Parallel to the Ring Plane in  $\text{Au}_{10}/\text{SPh}$  ( $n_{\parallel}$ ),  $\text{Au}_{10}/\text{SCH}_2\text{Ph}$  ( $n_{\parallel}$ ), and  $\text{Au}_{10}/\text{C}\equiv\text{CPh}$  ( $\pi_{\parallel}$ )<sup>a</sup>**

Cluster	MO, alpha
$\text{Au}_{10}/\text{SPh}$	 -5.532 eV (123a)
$\text{Au}_{10}/\text{SCH}_2\text{Ph}$	 -5.640 eV (127a)
$\text{Au}_{10}/\text{C}\equiv\text{CPh}$	 -5.723 eV (121a)

<sup>a</sup>The  $\alpha$  (spin-up) and  $\beta$  (spin-down) orbitals differ in energy by less than 0.1 eV. The results for the whole series of compounds ( $\text{Au}/\text{SPh}_n$ ,  $\text{Au}/\text{SCH}_2\text{Ph}_n$ , and  $\text{Au}_{10}/\text{C}\equiv\text{CPh}_n$ ,  $n = 1-3$ ) are shown in the Table S3.

the Supporting Information. We optimized the structures of the  $\text{SPh}_n$ ,  $\text{SCH}_2\text{Ph}_n$ , and  $\text{C}\equiv\text{CPh}_n$  compounds ( $n = 1-3$ ) attached to silver and gold cluster models.

The DFT results show that the highest occupied molecular orbital (HOMO) for both  $\text{Au}/\text{SPh}_n$  and  $\text{Au}/\text{C}\equiv\text{CPh}_n$  is partially delocalized; that is, although it is located predominantly on the anchoring group, it also includes contributions from the orbitals on the adjacent phenyl rings (Table 1). The values of the HOMO energies of the two molecules are comparable ( $-5.5 \text{ eV}$  for  $\text{SPh}_1$  and  $-5.7 \text{ eV}$  for  $\text{C}\equiv\text{CPh}_1$ ). The electronic structures of the conjugated systems differ from those of saturated  $n$ -alkylthiols, where the HOMO is localized on the anchoring atom (ca.  $-5.6 \text{ eV}$  for  $\text{Au}/\text{S}(\text{CH}_2)_n\text{CH}_3$ ) with little to no participation by orbitals on the adjacent atoms of the  $\text{CH}_2$  groups in the alkyl chain.<sup>1</sup>

Calculations on the  $\text{Au}_{10}/\text{C}\equiv\text{CPh}$  cluster illustrate the relevant interactions between the high-lying occupied orbitals of the conjugated molecular systems (Figure 3a), which include the  $\pi$  orbitals of the  $\text{C}\equiv\text{C}$  triple bond oriented both parallel ( $\pi_{\parallel}(\text{C}\equiv\text{C})$ ) and perpendicular to the ring plane ( $\pi_{\perp}(\text{C}\equiv\text{C})$ ) and the  $\pi$  orbitals of the benzene ring ( $\pi_{1a}(\text{Ph})$  and  $\pi_{1b}(\text{Ph})$ ). The  $\pi_{\parallel}(\text{C}\equiv\text{C})$  and  $\pi_{1a}(\text{Ph})$  orbitals have the same symmetry and show a strong interaction between the anchoring group and the phenyl  $\pi$  system; at the same time, because of their symmetries, the  $\pi_{\perp}(\text{C}\equiv\text{C})$  and  $\pi_{1b}(\text{Ph})$  orbitals remain localized on their respective moieties. The same trend is observed for the  $\text{Au}_{10}/\text{SPh}$  cluster but not for the  $\text{Au}_{10}/\text{SCH}_2\text{Ph}$  cluster (Figure S4). The presence of the methylene

spacer prevents the interaction between the anchoring group and phenyl  $\pi$  system even for the orbitals that have the same symmetry (Figure S4b). The  $\pi_{1a}(\text{Ph})$  orbitals of the phenyl rings interact strongly with each other in the  $\text{Au}/\text{C}\equiv\text{CPh}_n$ ,  $\text{Au}/\text{SCH}_2\text{Ph}_n$ , and  $\text{Au}/\text{SPh}_n$  series of compounds ( $n = 1-3$ ), as evidenced by their large energy splittings (Figure 3b–d).

The presence of a single methylene spacer in the  $\text{Au}/\text{SCH}_2\text{Ph}_n$  compounds ( $n = 1-3$ ), however, is sufficient to prevent the interaction between the  $n_{\parallel}(\text{S})$  lone-pair orbital of the anchoring group and the  $\pi_{1a}(\text{Ph})$  orbital of the phenyl  $\pi$  system, in contrast to the  $\text{Au}/\text{SPh}_n$  compounds ( $n = 1-3$ ) (Table 1). Disruption of the delocalization of orbitals from the anchoring groups onto the phenyl rings and the metal substrate (Table 1) is correlated with experimentally observed changes in the rate of charge transport (Figure 2). Specifically, the introduction of an insulating methylene spacer between the sulfur anchoring atom and the adjacent phenyl ring—a modification that generates  $\text{SCH}_2\text{Ph}_n$ —increases the attenuation factor across the molecule to  $\beta_{\text{Ag}} = 0.66 \text{ \AA}^{-1}$  and  $\beta_{\text{Au}} = 0.66 \text{ \AA}^{-1}$ , which are close to those for  $n$ -alkylthiolates on Ag and Au ( $\beta_{\text{Ag}} = 0.72 \text{ \AA}^{-1}$  and  $\beta_{\text{Au}} = 0.76 \text{ \AA}^{-1}$ ).<sup>2</sup> These values for  $\text{SCH}_2\text{Ph}_n$  are similar to that reported previously by us using a mercury junction ( $\beta_{\text{Ag}} = 0.66 \text{ \AA}^{-1}$ )<sup>48</sup> but somewhat higher than those reported by Frisbie and co-workers ( $\beta_{\text{Au}} = 0.41 \text{ \AA}^{-1}$ )<sup>47</sup> and Chiechi and co-workers ( $\beta_{\text{Au}} = 0.46 \text{ \AA}^{-1}$ )<sup>54</sup> for SAMs of  $\text{SCH}_2\text{Ph}_n$  on Au.

We investigated the influence of increasing the number of insulating  $\text{CH}_2$  groups from  $n = 1$  to  $n = 2$  and 3 on the current density (Figure S3). The values of  $J(V)$  measured for  $\text{S}(\text{CH}_2)_2\text{Ph}$ ,  $\text{S}(\text{CH}_2)_2\text{Ph}_2$ , and  $\text{S}(\text{CH}_2)_3\text{Ph}$  fit to the linear regression lines of the oligo(phenyl)methanethiols and  $n$ -alkylthiolates. These measurements indicate that the introduction of one insulating  $\text{CH}_2$  group between the anchoring atom and the adjacent phenyl ring has an influence on the electrical measurements similar to the influence of two and three  $\text{CH}_2$  groups (a conclusion reached previously for sulfur by Chiechi and co-workers).<sup>54</sup>

The data presented here for oligo(phenyl)methanethiols ( $\text{SCH}_2\text{Ph}_n$ ), phenylethylthiols ( $\text{S}(\text{CH}_2)_2\text{Ph}_n$ ,  $n = 1, 2$ ), and phenylpropylthiols ( $\text{S}(\text{CH}_2)_3\text{Ph}$ ) as well as those from our previous measurements on oligo(phenyl)carboxylates ( $\text{O}_2\text{CPh}_n$ ) on silver ( $\beta_{\text{Ag}} = 0.60 \text{ \AA}^{-1}$ )<sup>55</sup> indicate that disruption of the delocalization of orbitals from the bottom electrode and the anchoring group to the  $\text{Ph}_n$  group is correlated with values of  $\beta$  higher than those observed for SAMs of oligo(phenyl)thiolates ( $\text{SPh}_n$ ). In the case of oligo(phenyl)carboxylates, it is the presence of an orbital node on the carbon atom of the carboxylate group that disrupts the delocalization of orbitals from the  $\text{CO}_2^-$  group to the  $\text{Ph}_n$  moiety and produces an electronic effect similar to the presence of an intervening methylene group in  $\text{SCH}_2\text{Ph}_n$ . Additional studies on oligo(phenyl)carboxylates showed that decoupling the HOMO from strong interactions with the adjacent oligophenyl groups in the SAM allows the permutation of the order of electronically distinct functional groups in the junction. That is, the position of functional groups with different electronic properties (e.g.,  $\text{R}_1 = (\text{CH}_2)_n$  and  $\text{R}_2 = (\text{C}_6\text{H}_4)_m$ ) does not influence the overall rate of charge transport when the HOMO is localized on the anchoring group.<sup>56</sup>

## CONCLUSIONS

This study reports values of  $\beta$  and  $J_0$  (obtained using conical EGaIn top electrodes) for three series of aromatic SAMs

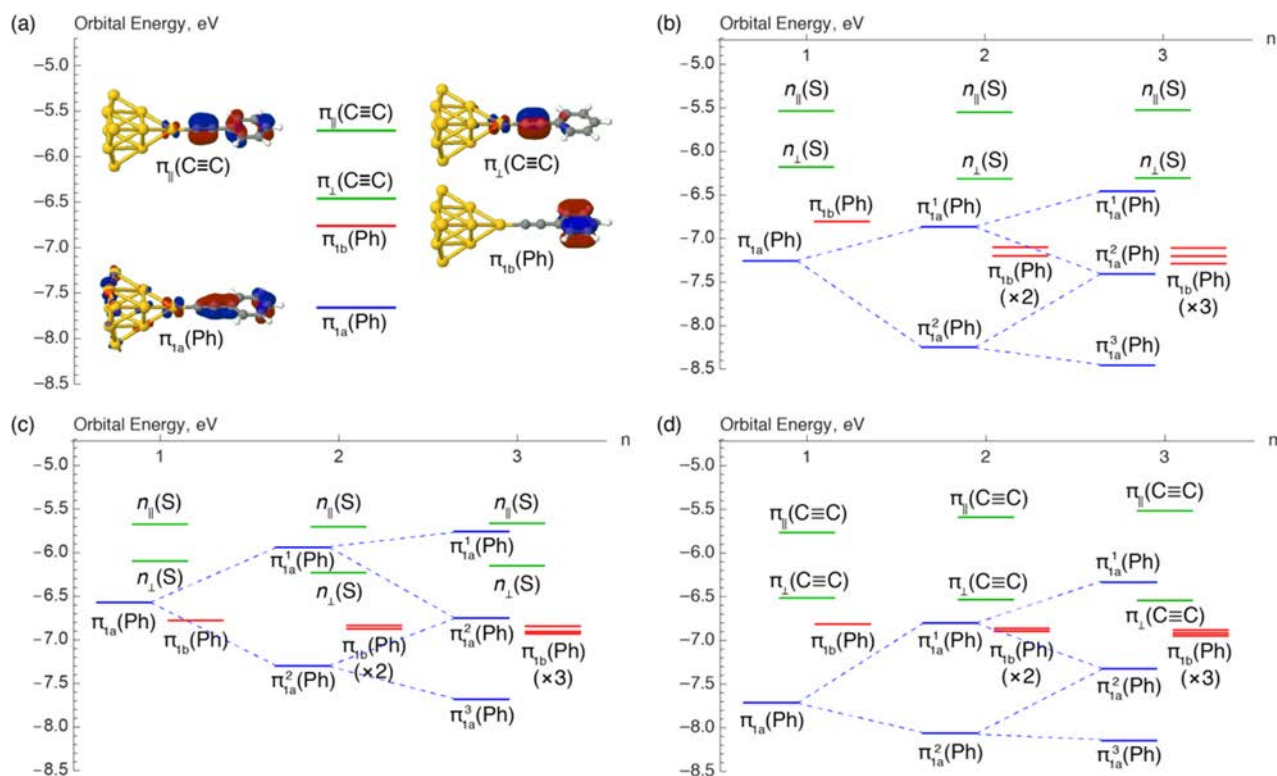


**Figure 3.** Orbital energy diagrams of high-lying occupied molecular orbitals in the Au/C≡CPh<sub>n</sub>, Au/SPh<sub>n</sub>, and Au/SCH<sub>2</sub>Ph<sub>n</sub> series ( $n = 1-3$ ). (a) Orbital energies and shapes of the high-lying occupied molecular orbitals in Au/C≡CPh. The energy levels of the  $\pi$  orbitals of the C≡C bond parallel ( $\pi_{\parallel}(\text{C}\equiv\text{C})$ ) and perpendicular ( $\pi_{\perp}(\text{C}\equiv\text{C})$ ) to the plane of the benzene ring are shown in green; the energy levels of the  $\pi$  orbitals of the phenyl ring ( $\pi_{1a}(\text{Ph})$  and  $\pi_{1b}(\text{Ph})$ ) are shown in blue and red, respectively; only the shapes of the  $\alpha$  (spin-up) orbitals are shown. (b-d) Orbital energy diagrams of the (b) Au/SPh<sub>n</sub>, (c) Au/SCH<sub>2</sub>Ph<sub>n</sub>, and (d) Au/C≡CPh<sub>n</sub> series of compounds ( $n = 1-3$ ).

(SPh<sub>n</sub>, SCH<sub>2</sub>Ph<sub>n</sub>, and C≡CCH<sub>2</sub>Ph<sub>n</sub>) on gold and silver substrates. These results demonstrate significant sensitivity of the tunneling current through these junctions to the molecular and electronic structures of the interface between the metal (Au or Ag) bottom electrode and the SAM; others (Frisbie, Chiechi, Tokumoto, Bjørnholm, and co-workers)<sup>47,54,57,58</sup> also concluded that tunneling currents are sensitive to the characteristics of the interfaces. At least in the systems described here, this sensitivity seems to be based largely on the extent of delocalization of the HOMO—here, an orbital centered on –SR or –C≡CR—onto the proximate parts of the SAM. The magnitude of this sensitivity is clear from a comparison of two observations.

- The value of the attenuation of the tunneling current with distance ( $\beta$ ) is indistinguishable for SAMs of SPh<sub>n</sub> and C≡CPh<sub>n</sub> on gold. These two series of SAMs have substantially different anchoring groups (–S– vs –C≡C–) but both are characterized by the delocalization of high-lying orbitals between the anchoring group and the adjacent phenyl rings.
- The introduction of a single CH<sub>2</sub> group between the aromatic group and the sulfur anchoring atom—generating SCH<sub>2</sub>Ph<sub>n</sub>—increases  $\beta$  to a value very similar to that of a length-matched saturated aliphatic SAM. We attribute this increase in  $\beta$  to a disruption in the delocalization of orbitals from the anchoring group to the phenyl rings.

In addition to characterizing the rates of charge transport across a series of oligophenyls that have structurally distinct interfaces with the bottom electrode, this study highlights some

important features of the tunneling barrier that went undetected in earlier studies using insulating alkanethiolates with a localized HOMO on the anchoring sulfur atom. Our previous investigations of the influence of the metal/SAM interface on the rate of charge transport considered alkyl-based SAMs having anchoring groups (e.g., SR, C≡CR, and O<sub>2</sub>CR)<sup>49</sup> in which the HOMO (centered on the anchoring group) was not delocalized into the R = (CH<sub>2</sub>)<sub>n</sub>H group. On the basis of the indistinguishable values of  $\beta$  and  $J_0$ , that study suggested that the interface between the metal and the SAM is not important in determining the rate of charge transport in junctions of the structure M/A(CH<sub>2</sub>)<sub>n</sub>H//Ga<sub>2</sub>O<sub>3</sub>/EGaIn, where A is the “anchoring group” (e.g., S, C≡C, O<sub>2</sub>C).<sup>59</sup> The current study analyzed conjugated molecular systems where the HOMO extends beyond the anchoring group and onto the adjacent phenyl rings and established that interfaces characterized by high-lying occupied molecular orbitals that are localized and delocalized are quite different. Furthermore, changes in the molecular structure of the interface that disrupt the delocalization of the HOMO increase the value of  $\beta$ .

## ■ ASSOCIATED CONTENT

### ● Supporting Information

The Supporting Information is available free of charge on the ACS Publications website at DOI: 10.1021/acs.jpcc.6b01253.

Detailed experimental and computational procedures, histograms of current densities, and summary of junction measurements (PDF)

## ■ AUTHOR INFORMATION

## Corresponding Author

\*Tel: 617-495-9430. Fax: 617-495-9857. E-mail: [gwhitesides@gmgroup.harvard.edu](mailto:gwhitesides@gmgroup.harvard.edu)

## Notes

The authors declare no competing financial interest.

## ■ ACKNOWLEDGMENTS

The measurements of rates of charge transport and the preparation of the SAMs were supported by a subcontract from Northwestern University from the United States Department of Energy (DOE) (DE-SC0000989). This work was also partially funded by the National Science Foundation (NSF) award CHE-1506993. The National Science Centre Poland (Grant DEC-2013/10/E/ST5/00060) supported the spectroscopic studies of the SAMs and the development of the method for preparing SAMs with structure  $\text{Au}_6\text{C}\equiv\text{CR}$ . The DOE grant from Northwestern also supported the salaries of C.M.B, M.B., F.C.S., and K.-C.L. The Simons Foundation (Award 290364) supported the salary of S.N.S. The Cyberdiscovery Initiative Type II (CDI2) Grant from the National Science Foundation (NSF) (OIA-1125087) supported the salary for D.R. Sample characterization was performed at the Center for Nanoscale Systems (CNS) at Harvard University, a member of the National Nanotechnology Infrastructure Network (NNIN), which is supported by NSF (ECS-0335765). In particular, we appreciate the assistance of Dr. Hao-Yu Lin at CNS. We thank Dr. Benjamin Breiten for his assistance in the synthesis of terphenylacetylene.

## ■ REFERENCES

- (1) Mirjani, F.; Thijssen, J. M.; Whitesides, G. M.; Ratner, M. A. Charge Transport Across Insulating Self-Assembled Monolayers: Non-equilibrium Approaches and Modeling To Relate Current and Molecular Structure. *ACS Nano* **2014**, *8*, 12428–12436.
- (2) Baghbanzadeh, M.; Simeone, F. C.; Bowers, C. M.; Liao, K. C.; Thuo, M.; Baghbanzadeh, M.; Miller, M. S.; Carmichael, T. B.; Whitesides, G. M. Odd-Even Effects in Charge Transport across n-Alkanethiolate-Based SAMs. *J. Am. Chem. Soc.* **2014**, *136*, 16919–16925.
- (3) Toledano, T.; Sazan, H.; Mukhopadhyay, S.; Alon, H.; Lerman, K.; Bendikov, T.; Major, D. T.; Sukenik, C. N.; Vilan, A.; Cahen, D. Odd-Even Effect in Molecular Electronic Transport via an Aromatic Ring. *Langmuir* **2014**, *30*, 13596–13605.
- (4) Nurbawono, A.; Liu, S. L.; Nijhuis, C. A.; Zhang, C. Odd-Even Effects in Charge Transport through Self-Assembled Monolayer of Alkanethiolates. *J. Phys. Chem. C* **2015**, *119*, 5657–5662.
- (5) Jiang, L.; Sangeeth, C. S.; Nijhuis, C. A. The Origin of the Odd-Even Effect in the Tunneling Rates across EGaIn Junctions with Self-Assembled Monolayers (SAMs) of n-Alkanethiolates. *J. Am. Chem. Soc.* **2015**, *137*, 10659–10667.
- (6) Yuan, L.; Thompson, D.; Cao, L.; Nerngchangnong, N.; Nijhuis, C. A. One Carbon Matters: The Origin and Reversal of Odd-Even Effects in Molecular Diodes with Self-Assembled Monolayers of Ferrocenyl-Alkanethiolates. *J. Phys. Chem. C* **2015**, *119*, 17910–17919.
- (7) Liao, K. C.; Bowers, C. M.; Yoon, H. J.; Whitesides, G. M. Fluorination, and Tunneling across Molecular Junctions. *J. Am. Chem. Soc.* **2015**, *137*, 3852–3858.
- (8) Nerngchangnong, N.; Yuan, L.; Qi, D. C.; Li, J.; Thompson, D.; Nijhuis, C. A. The Role of van der Waals Forces in the Performance of Molecular Diodes. *Nat. Nanotechnol.* **2013**, *8*, 113–118.
- (9) Yuan, L.; Nerngchangnong, N.; Cao, L.; Hamoudi, H.; del Barco, E.; Roemer, M.; Sriramula, R. K.; Thompson, D.; Nijhuis, C. A. Controlling the Direction of Rectification in a Molecular Diode. *Nat. Commun.* **2015**, *6*, 6324.
- (10) Yoon, H. J.; Liao, K. C.; Lockett, M. R.; Kwok, S. W.; Baghbanzadeh, M.; Whitesides, G. M. Rectification in Tunneling Junctions: 2,2'-Bipyridyl-Terminated n-Alkanethiolates. *J. Am. Chem. Soc.* **2014**, *136*, 17155–17162.
- (11) Cohen, R.; Stokbro, K.; Martin, J. M. L.; Ratner, M. A. Charge Transport in Conjugated Aromatic Molecular Junctions: Molecular Conjugation and Molecule-Electrode Coupling. *J. Phys. Chem. C* **2007**, *111*, 14893–14902.
- (12) Choi, S. H.; Kim, B.; Frisbie, C. D. Electrical Resistance of Long Conjugated Molecular Wires. *Science* **2008**, *320*, 1482–1486.
- (13) Kim, B.; Beebe, J. M.; Jun, Y.; Zhu, X. Y.; Frisbie, C. D. Correlation between HOMO Alignment and Contact Resistance in Molecular Junctions: Aromatic Thiols versus Aromatic Isocyanides. *J. Am. Chem. Soc.* **2006**, *128*, 4970–4971.
- (14) Wu, S. M.; Gonzalez, M. T.; Huber, R.; Grunder, S.; Mayor, M.; Schönenberger, C.; Calame, M. Molecular Junctions Based on Aromatic Coupling. *Nat. Nanotechnol.* **2008**, *3*, 569–574.
- (15) Peng, G.; Strange, M.; Thygesen, K. S.; Mavrikakis, M. Conductance of Conjugated Molecular Wires: Length Dependence, Anchoring Groups, and Band Alignment. *J. Phys. Chem. C* **2009**, *113*, 20967–20973.
- (16) Quek, S. Y.; Choi, H. J.; Louie, S. G.; Neaton, J. B. Length Dependence of Conductance in Aromatic Single-Molecule Junctions. *Nano Lett.* **2009**, *9*, 3949–3953.
- (17) Yaffe, O.; Qi, Y. B.; Scheres, L.; Puniredd, S. R.; Segev, L.; Ely, T.; Haick, H.; Zuilhof, H.; Vilan, A.; Kronik, L.; Kahn, A.; Cahen, D. Charge Transport across Metal/Molecular (Alkyl) Monolayer-Si Junctions is Dominated by the LUMO Level. *Phys. Rev. B: Condens. Matter Mater. Phys.* **2012**, *85*, 045433.
- (18) Launay, J. P. Long-Distance Intervalence Electron Transfer. *Chem. Soc. Rev.* **2001**, *30*, 386–397.
- (19) Lu, Q.; Liu, K.; Zhang, H. M.; Du, Z. B.; Wang, X. H.; Wang, F. S. From Tunneling to Hopping: A Comprehensive Investigation of Charge Transport Mechanism in Molecular Junctions Based on Oligo(p-phenylene ethynylene)s. *ACS Nano* **2009**, *3*, 3861–3868.
- (20) Hoeben, F. J. M.; Jonkheijm, P.; Meijer, E. W.; Schenning, A. P. H. J. About Supramolecular Assemblies of  $\pi$ -Conjugated Systems. *Chem. Rev.* **2005**, *105*, 1491–1546.
- (21) Bergren, A. J.; McCreery, R. L.; Stoyanov, S. R.; Gusarov, S.; Kovalenko, A. Electronic Characteristics and Charge Transport Mechanisms for Large Area Aromatic Molecular Junctions. *J. Phys. Chem. C* **2010**, *114*, 15806–15815.
- (22) Hamoudi, H.; Neppl, S.; Kao, P.; Schupbach, B.; Feulner, P.; Terfort, A.; Allara, D.; Zharnikov, M. Orbital-Dependent Charge Transport Dynamics in Conjugated Self-Assembled Monolayers. *Phys. Rev. Lett.* **2011**, *107*, 027801.
- (23) Dell, E. J.; Capozzi, B.; DuBay, K. H.; Berkelbach, T. C.; Moreno, J. R.; Reichman, D. R.; Venkataraman, L.; Campos, L. M. Impact of Molecular Symmetry on Single-Molecule Conductance. *J. Am. Chem. Soc.* **2013**, *135*, 11724–11727.
- (24) Sachs, S. B.; Dudek, S. P.; Hsung, R. P.; Sita, L. R.; Smalley, J. F.; Newton, M. D.; Feldberg, S. W.; Chidsey, C. E. D. Rates of Interfacial Electron Transfer through  $\pi$ -Conjugated Spacers. *J. Am. Chem. Soc.* **1997**, *119*, 10563–10564.
- (25) Lei, T.; Dou, J. H.; Cao, X. Y.; Wang, J. Y.; Pei, J. Electron-Deficient Poly(p-phenylene vinylene) Provides Electron Mobility over  $1\text{ cm}^2\text{ V}^{-1}\text{ s}^{-1}$  under Ambient Conditions. *J. Am. Chem. Soc.* **2013**, *135*, 12168–12171.
- (26) Simmons, J. G. Generalized Formula for Electric Tunnel Effect between Similar Electrodes Separated by a Thin Insulating Film. *J. Appl. Phys.* **1963**, *34*, 1793–1803.
- (27) Heimel, G.; Romaner, L.; Bredas, J. L.; Zojer, E. Odd-Even Effects in Self-Assembled Monolayers of omega-(Biphenyl-4-yl)-alkanethiols: A First-Principles Study. *Langmuir* **2008**, *24*, 474–482.
- (28) Heimel, G.; Rissner, F.; Zojer, E. Modeling the Electronic Properties of  $\pi$ -Conjugated Self-Assembled Monolayers. *Adv. Mater.* **2010**, *22*, 2494–2513.
- (29) Kong, L. M.; Chesneau, F.; Zhang, Z. Z.; Staier, F.; Terfort, A.; Dowben, P. A.; Zharnikov, M. Electronic Structure of Aromatic

Monomolecular Films: The Effect of Molecular Spacers and Interfacial Dipoles. *J. Phys. Chem. C* **2011**, *115*, 22422–22428.

(30) Frey, S.; Stadler, V.; Heister, K.; Eck, W.; Zharnikov, M.; Grunze, M.; Zeysing, B.; Terfort, A. Structure of Thioaromatic Self-Assembled Monolayers on Gold and Silver. *Langmuir* **2001**, *17*, 2408–2415.

(31) Ishida, T.; Mizutani, W.; Azebara, H.; Miyake, K.; Aya, Y.; Sasaki, S.; Tokumoto, H. Molecular Arrangement and Electrical Conduction of Self-Assembled Monolayers Made from Terphenyl Thiols. *Surf. Sci.* **2002**, *514*, 187–193.

(32) de Boer, B.; Meng, H.; Perepichka, D. F.; Zheng, J.; Frank, M. M.; Chabal, Y. J.; Bao, Z. N. Synthesis and Characterization of Conjugated Mono- and Dithiol Oligomers and Characterization of Their Self-Assembled Monolayers. *Langmuir* **2003**, *19*, 4272–4284.

(33) Tour, J. M.; Jones, L.; Pearson, D. L.; Lamba, J. J. S.; Burgin, T. P.; Whitesides, G. M.; Allara, D. L.; Parikh, A. N.; Atre, S. V. Self-Assembled Monolayers and Multilayers of Conjugated Thiols, Alpha, Omega-Dithiols, and Thioacetyl-Containing Adsorbates - Understanding Attachments between Potential Molecular Wires and Gold Surfaces. *J. Am. Chem. Soc.* **1995**, *117*, 9529–9534.

(34) Kronemeijer, A. J.; Huisman, E. H.; Akkerman, H. B.; Goossens, A. M.; Katsouras, I.; van Hal, P. A.; Geuns, T. C. T.; van der Molen, S. J.; Blom, P. W. M.; de Leeuw, D. M. Electrical Characteristics of Conjugated Self-Assembled Monolayers in Large-Area Molecular Junctions. *Appl. Phys. Lett.* **2010**, *97*, 173302.

(35) Shaporenko, A.; Elbing, M.; Blaszczyk, A.; von Hanisch, C.; Mayor, M.; Zharnikov, M. Self-Assembled Monolayers from Biphenyldithiol Derivatives: Optimization of the Deprotection Procedure and Effect of the Molecular Conformation. *J. Phys. Chem. B* **2006**, *110*, 4307–4317.

(36) Grave, C.; Risko, C.; Shaporenko, A.; Wang, Y. L.; Nuckolls, C.; Ratner, M. A.; Rampi, M. A.; Zharnikov, M. Charge Transport through Oligoarylene Self-Assembled Monolayers: Interplay of Molecular Organization, Metal-Molecule Interactions, and Electronic Structure. *Adv. Funct. Mater.* **2007**, *17*, 3816–3828.

(37) Heister, K.; Zharnikov, M.; Grunze, M.; Johansson, L. S. O. Adsorption of Alkanethiols and Biphenylthiols on Au and Ag Substrates: A High-Resolution X-ray Photoelectron Spectroscopy Study. *J. Phys. Chem. B* **2001**, *105*, 4058–4061.

(38) Himmel, H. J.; Terfort, A.; Woll, C. Fabrication of a Carboxyl-Terminated Organic Surface with Self-Assembly of Functionalized Terphenylthiols: The Importance of Hydrogen Bond Formation. *J. Am. Chem. Soc.* **1998**, *120*, 12069–12074.

(39) Maity, P.; Takano, S.; Yamazoe, S.; Wakabayashi, T.; Tsukuda, T. Binding Motif of Terminal Alkynes on Gold Clusters. *J. Am. Chem. Soc.* **2013**, *135*, 9450–9457.

(40) Ford, M. J.; Hoft, R. C.; McDonagh, A. Theoretical Study of Ethynylbenzene Adsorption on Au(111) and Implications for a New Class of Self-Assembled Monolayer. *J. Phys. Chem. B* **2005**, *109*, 20387–20392.

(41) McDonagh, A. M.; Zareie, H. M.; Ford, M. J.; Barton, C. S.; Ginic-Markovic, M.; Matison, J. G. Ethynylbenzene Monolayers on Gold: A Metal-Molecule Binding Motif Derived from a Hydrocarbon. *J. Am. Chem. Soc.* **2007**, *129*, 3533–3538.

(42) Pla-Vilanova, P.; Aragones, A. C.; Ciampi, S.; Sanz, F.; Darwish, N.; Diez-Perez, I. The Spontaneous Formation of Single-Molecule Junctions via Terminal Alkynes. *Nanotechnology* **2015**, *26*, 381001.

(43) Zaba, T.; Noworolska, A.; Bowers, C. M.; Breiten, B.; Whitesides, G. M.; Cyganik, P. Formation of Highly Ordered Self-Assembled Monolayers of Alkynes on Au(111) Substrate. *J. Am. Chem. Soc.* **2014**, *136*, 11918–11921.

(44) Simmons, J. G. Electric Tunnel Effect between Dissimilar Electrodes Separated by a Thin Insulating Film. *J. Appl. Phys.* **1963**, *34*, 2581–2590.

(45) Simmons, J. G.; Unterkofler, G. J. Potential Barrier Shape Determination in Tunnel Junctions. *J. Appl. Phys.* **1963**, *34*, 1828.

(46) Simeone, F. C.; Yoon, H. J.; Thuo, M. M.; Barber, J. R.; Smith, B.; Whitesides, G. M. Defining the Value of Injection Current and

Effective Electrical Contact Area for EGaIn-Based Molecular Tunneling Junctions. *J. Am. Chem. Soc.* **2013**, *135*, 18131–18144.

(47) Wold, D. J.; Haag, R.; Rampi, M. A.; Frisbie, C. D. Distance Dependence of Electron Tunneling through Self-Assembled Monolayers Measured by Conducting Probe Atomic Force Microscopy: Unsaturated versus Saturated Molecular Junctions. *J. Phys. Chem. B* **2002**, *106*, 2813–2816.

(48) Holmlin, R. E.; Haag, R.; Chabinc, M. L.; Ismagilov, R. F.; Cohen, A. E.; Terfort, A.; Rampi, M. A.; Whitesides, G. M. Electron Transport through Thin Organic Films in Metal-Insulator-Metal Junctions Based on Self-Assembled Monolayers. *J. Am. Chem. Soc.* **2001**, *123*, 5075–5085.

(49) Holmlin, R. E.; Ismagilov, R. F.; Haag, R.; Mujica, V.; Ratner, M. A.; Rampi, M. A.; Whitesides, G. M. Correlating Electron Transport and Molecular Structure in Organic Thin Films. *Angew. Chem., Int. Ed.* **2001**, *40*, 2316–2320.

(50) Anariba, F.; McCreery, R. L. Electronic Conductance Behavior of Carbon-Based Molecular Junctions with Conjugated Structures. *J. Phys. Chem. B* **2002**, *106*, 10355–10362.

(51) Kaligned, V.; Moreno-Garcia, P.; Valkenier, H.; Hong, W.; Garcia-Suarez, V. M.; Buitter, P.; Otten, J. L.; Hummelen, J. C.; Lambert, C. J.; Wandlowski, T. Correlations between Molecular Structure and Single-Junction Conductance: a Case Study with Oligo(phenylene-ethynylene)-Type Wires. *J. Am. Chem. Soc.* **2012**, *134*, 5262–5275.

(52) Querebillo, C. J.; Terfort, A.; Allara, D. L.; Zharnikov, M. Static Conductance of Nitrile-Substituted Oligophenylene and Oligo(phenylene ethynylene) Self-Assembled Mono layers Studied by the Mercury-Drop Method. *J. Phys. Chem. C* **2013**, *117*, 25556–25561.

(53) Masillamani, A. M.; Crivillers, N.; Orgiu, E.; Rotzler, J.; Bossert, D.; Thippeswamy, R.; Zharnikov, M.; Mayor, M.; Samori, P. Multiscale Charge Injection and Transport Properties in Self-Assembled Monolayers of Biphenyl Thiols with Varying Torsion Angles. *Chem. - Eur. J.* **2012**, *18*, 10335–10347.

(54) Fracasso, D.; Muglali, M. I.; Rohwerder, M.; Terfort, A.; Chiechi, R. C. Influence of an Atom in EGaIn/Ga<sub>2</sub>O<sub>3</sub> Tunneling Junctions Comprising Self-Assembled Monolayers. *J. Phys. Chem. C* **2013**, *117*, 11367–11376.

(55) Liao, K.-C.; Yoon, H. J.; Bowers, C. M.; Simeone, F. C.; Whitesides, G. M. Replacing Ag<sup>TS</sup>SCH<sub>2</sub>-R with Ag<sup>TS</sup>O<sub>2</sub>-C-R in EGaIn-based Tunneling Junctions Does Not Significantly Change Rates of Charge Transport. *Angew. Chem., Int. Ed.* **2014**, *53*, 3889–3893.

(56) Liao, K. C.; Hsu, L. Y.; Bowers, C. M.; Rabitz, H.; Whitesides, G. M. Molecular Series-Tunneling Junctions. *J. Am. Chem. Soc.* **2015**, *137*, 5948–5954.

(57) Ishida, T.; Mizutani, W.; Aya, Y.; Ogiso, H.; Sasaki, S.; Tokumoto, H. Electrical Conduction of Conjugated Molecular SAMs Studied by Conductive Atomic Force Microscopy. *J. Phys. Chem. B* **2002**, *106*, 5886–5892.

(58) Danilov, A.; Kubatkin, S.; Kafanov, S.; Hedegard, P.; Stuhr-Hansen, N.; Moth-Poulsen, K.; Bjornholm, T. Electronic Transport in Single Molecule Junctions: Control of the Molecule-Electrode Coupling through Intramolecular Tunneling Barriers. *Nano Lett.* **2008**, *8*, 1–5.

(59) Bowers, C. M.; Liao, K. C.; Zaba, T.; Rappoport, D.; Baghbanzadeh, M.; Breiten, B.; Krzykawska, A.; Cyganik, P.; Whitesides, G. M. Characterizing the Metal-SAM Interface in Tunneling Junctions. *ACS Nano* **2015**, *9*, 1471–1477.